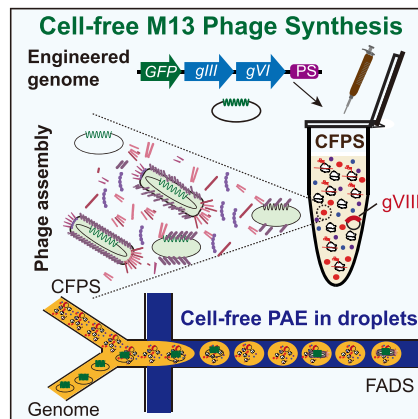


Report

A cell-free bacteriophage synthesis system for directed evolution



This study introduces a robust cell-free synthesis method for M13 phage, enhanced by genome optimization and multicopy protein presynthesis. This approach facilitates the rapid and substantial production of M13 phage and supports phage-assisted evolution within droplets. These innovations significantly advance the frontiers of functional phage synthesis and *in vitro* screening.

Bo Xu (许波), Li-Hua Liu (刘丽花), Houliang Lin (林厚良), Yang Zhang (张洋), Ying Huang (黄盈), Qing He (何青), Fan Wang (王帆), Yi-Rui Wu (吴奕瑞), Zhiqian Zhang (张志乾), Ao Jiang (江翱)

xub@whu.edu.cn (B. Xu),
worthy@tidetronbio.com (Z. Zhang)
jiangao@tidetronbio.com (A. Jiang).

Highlights

We developed an improved cell-free synthesis method for the rapid and substantial production of M13 phage.

Genome simplification and high-copy origin of replication substantially increased the efficiency of cell-free synthesis.






A cell-free system in droplets broadened the applicability of phage-assisted evolution.

Fluorescence-activated sorting markedly improved the evolutionary efficiency in droplets.

Trends in Biotechnology, Month 2024,
Vol. xx, No. xx
<https://doi.org/10.1016/j.tibtech.2024.10.005>

Report

A cell-free bacteriophage synthesis system for directed evolution

Bo Xu ^{1,3,*}, Li-Hua Liu ^{2,3}, Houliang Lin ^{2,3}, Yang Zhang ^{2,3}, Ying Huang (黄盈)^{2,3}, Qing He (何青)^{2,3}, Fan Wang (王帆)^{2,3}, Yi-Rui Wu (吴奕瑞)^{2,3}, Zhigian Zhang (张志乾)^{2,3,*}, and Ao Jiang ^{2,3,4,*}

Efficient phage production has always been an urgent need in fields such as drug discovery, disease treatment, and gene evolution. To meet this demand, we constructed a robust cell-free synthesis system for generating M13 phage by simplifying its genome, enabling a three-times faster efficiency compared with the traditional method *in vivo*. We further developed a cell-free directed evolution system in droplets, comprising a modified helper plasmid (Δ PS- Δ gIII- Δ gVI) and the simplified M13 genome-carrying gene mutation library. This system was greatly improved when coupled with fluorescence-activated droplet sorting (FADS). We successfully evolved the T7 RNA polymerase (RNAP), achieving a twofold higher activity to read through the T7 terminator. Moreover, we evolved the tryptophan tRNA into a suppressor tRNA with an eightfold increase in activity to read through the stop codon UAG.

Introduction

Given their ability to infect and replicate within bacterial hosts, bacteriophages, also known as phages, receive significant interest for applications in various fields, such as medical therapeutics [1,2], peptide drug screening [3,4], industrial food production [5], as well as directed evolution of genes of interest (GOI) [6–8]. However, the host dependency of phages constrains their scalability and presents formidable challenges in phage preparation, particularly within the context of **phage-assisted evolution (PAE)** (see [Glossary](#)). To overcome these challenges, researchers recently directed their efforts toward using **cell-free synthesis systems** for efficient *in vitro* production of phages, including T7, psf-2, and phiES15 [9,10], whereas a focus on the M13 phage has been lacking.

The M13 phage has several distinctive properties that set it apart from other commonly studied phages. It is a filamentous phage belonging to the Inoviridae, distinguished by a unique lifecycle characterized by a delicate balance between viral replication and host survival [11,12]. Its genome, a covalently closed circular single-stranded DNA (ssDNA), ~6.4 kb in length, encodes a limited number of genes, facilitating its efficient replication in a rolling circle manner and assembly within the bacterial host [6,11]. It primarily comprises a genome encapsulated within a protein coat, ~99% of which is formed by protein VIII, rendering M13 the longest phage reported thus far [11]. While this attribute enhances the utility of M13 for phage display technology by offering substantial display sites [3,4], it also presents significant challenges for its *in vitro* synthesis and assembly processes.

The lifecycle of M13 begins with the attachment of the phage to its bacterial host, typically *Escherichia coli*, mediated by surface protein III (pIII). Once attached, M13 injects its genome

Technology readiness

The cell-free M13 phage synthesis system presented in this study has achieved a Technology Readiness Level (TRL) of 4, signifying its successful validation in laboratory conditions through the utilization of meticulously engineered M13 genomic DNA. While our optimization strategy for M13 genomic DNA has demonstrated the potential to substantially augment the synthesis capabilities of cell-free platforms for M13 phage, several challenges remain to be resolved before full-scale implementation. These challenges encompass the strategic allocation and precise regulation of M13 gene expression, the enhancement of *in vitro* assembly efficiency for phages, and augmentation of the stability and infectivity of the assembled phages. To overcome these challenges, the development of more efficient and streamlined cell-free synthesis systems and gene expression control technologies is imperative. This will ensure the fulfillment of the intricate requirements for *in vitro* phage synthesis and assembly, optimize the efficiency of raw material utilization, and enhance phage yield. Furthermore, the cell-free PAE technology confronts the challenge of ensuring evolutionary continuity. Coupling the GOI activity with the replication process of phage genomes could serve as an effective strategy to mitigate this limitation.

Upon fulfillment of these readiness criteria, the cell-free M13 phage synthesis system will be recognized as a potential method for the large-scale production of M13 phage, and as a formidable approach for broadening the scope of directed evolution technology applications.

¹School of Basic Medical Sciences, Hubei University of Science and Technology, Xianning 437100, PR China

into the host cell to serve as a template for both replication and transcription [6]. One of the defining features is its ability to replicate in the host cell without causing cell lysis, which it achieves using a mechanism to extrude its replicated DNA through the bacterial membrane, allowing its continuous replication and propagation [11].

Given these distinctive attributes of M13 phage and its broad applications in fields such as phage display, biosensing, vaccine development, gene therapy, and directed evolution [11,12], establishing an expeditious synthesis method for M13 phage is desirable. Thus, this investigation aimed to develop a cell-free synthesis approach for M13 phage and to leverage this approach to optimize PAE technology.

Results

Improving a cell-free synthesis system for quick and robust preparation of M13 phage

We hypothesized that a cell-free protein synthesis (CFPS) system [9,10] could be used to generate and assemble the M13 phage *in vitro*, since the M13 phage only contains 11 genes, which are relatively straightforward to synthesize [10]. To verify this hypothesis, we extracted the cell contents of *E. coli* JM109 to synthesize the M13 phage by adding either phage granules or its genomic DNA (Figure 1A). The results showed that the phage titer increased over time, with higher titers achieved with the genomic DNA rather than with complete granules, although both were lower compared with *in vivo* synthesis. The titer plateaued at 10^5 plaque-forming unit (pfu)/ml at 12 h (Figure 1B), far less than the requirements of the application for directed evolution.

Given that the CFPS system performed better using genomic DNA compared with complete granules, we determined the optimal concentration of genomic DNA for massive phage generation. The results demonstrated that phage synthesis increased with increasing DNA input, and reached a plateau at a concentration of 100 ng/ μ l (Figure 1C). Moreover, a concentration <0.1 ng/ μ l led to an almost undetectable phage titer in the CFPS system, demonstrating the

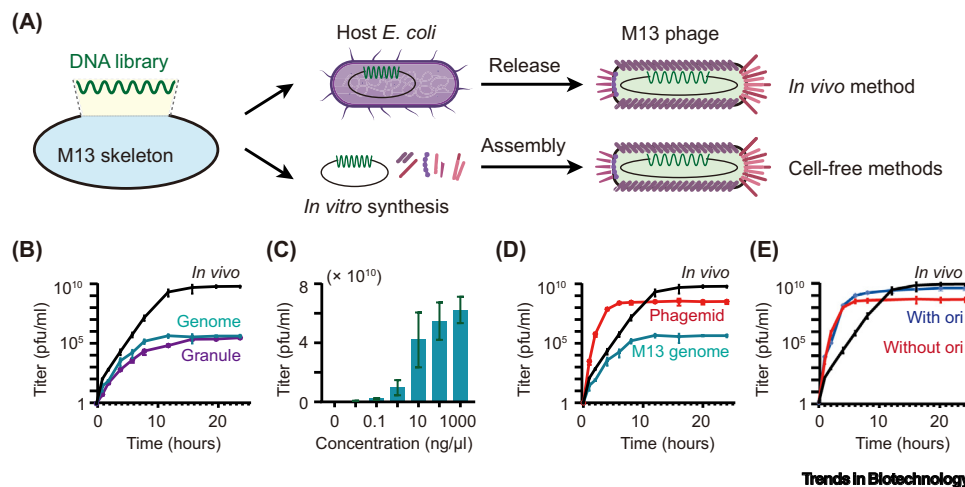


Figure 1. Optimization of a cell-free phage production system for robust phage preparation. (A) Phage preparation using a traditional *in vivo* method and a cell-free synthesis system in droplets. (B) Changes in M13 phage titer achieved by three synthesis systems. (C) Synthesis ability of M13 phage under different concentrations of genomic DNA (0.01–1000 ng/ μ l). (D) Changes in phage titer *in vivo* and in a cell-free system containing either the completed M13 genome or the simplified phagemid. (E) Changes in phage titer *in vivo* and in the cell-free system containing phagemid with or without the pMB1 origin of replication (ori). Error bars represent mean \pm standard deviation (SD) values. Abbreviations: *E. coli*, *Escherichia coli*; pfu, plaque forming unit.

²Tidetron Bioworks Technology (Guangzhou) Co., Ltd, Guangzhou Qianxiang Bioworks Co., Ltd., Guangzhou, Guangdong 510000, PR China

³All authors contributed equally to this work

⁴Lead contact

*Correspondence: xub@whu.edu.cn (B. Xu), worthy@tidetronbio.com (Z. Zhang), and jiangao@tidetronbio.com (A. Jiang).

minimum genome input required for directed evolution (Figure 1C). These findings suggest that the M13 phage can be synthesized and assembled in the CFPS system.

To further improve the efficiency of phage synthesis *in vitro*, we simplified the phage genome according to previous reports, to alleviate the pressure of unnecessary gene expression [12,13]. The resulting modified helper phage (HP) plasmid (M13KO7-ΔPS-ΔgIII-ΔgVI) contained the kanamycin-resistance gene (*KanR*) and almost all propagation-required genes except genes III (*gIII*), VI (*gVI*), and the **M13 packaging signal (PS)**, to inhibit phage propagation on HP. The HP plasmid was transformed into *E. coli* JM109 to synthesize in advance these phage propagation-related genes carried by the plasmid. This phage–plasmid hybrid (phagemid) constitutively expressed PS, *gIII*, and *gVI*. Subsequently, we extracted the cell contents from *E. coli* JM109 containing HP, and determined phage production by adding phagemid. The results showed that the simplified phagemid significantly enhanced the production speed and yield of phage. The titer reached a plateau of 10^8 pfu/ml at 3 h, markedly quicker than *in vivo* generation (Figure 1D). These results indicate that this CFPS system can efficiently generate and assemble the functional M13 phage.

Subsequently, to maximize the use of material resources in the host cell, we inserted a high-copy **origin of replication (ori)** pMB1 from the pUC19 plasmid into the HP to increase the proportion of products required for phage proliferation in the cell lysate. When carrying the pMB1 ori, which is reported to be the highest copy number of ori, the titer of M13 phage in the cell-free system reached a plateau of $>10^9$ pfu/ml, which was only slightly lower than the yield *in vivo* (Figure 1E). Moreover, the phage generation rate in the cell-free system was two to three times greater than that *in vivo* (Figure 1E).

Developing a cell-free PAE method in droplets

Although we achieved rapid and efficient M13 phage preparation in the cell-free system, it was still not suitable for directed evolution of the GOI due to a lack of independent evolutionary space, given that the genome DNA mutations should be specifically packaged to the corresponding phenotypic individuals during screening. To achieve this, we utilized the cell-free synthesis system for M13 phage in microdroplets. A GFP gene was inserted into the phagemid to visualize phage synthesis (Figure 2A). Next, we determined the DNA input to generate M13 phage in droplets. Based on the results, an optimal concentration of 1.5–2.5 ng/ml phagemid was chosen to be embedded with the cell contents of *E. coli* JM109 to ensure that 10–20% of droplets contained phage production to avoid polyclonal interference (Figure 2B).

Given that the fluorescence intensity of GFP visualizes phage synthesis, we utilized **FADS** [14] to obtain the droplets, the contents of which contributed to the synthesis of M13 phage (Video S1 in the supplemental information online). To test the efficiency of droplet sorting for phage generation, we mixed the phagemids with or without the *GFP* gene equally, and then added the mixture to the cell-free system for droplet preparation. Approximately one-sixth of the droplets exhibited GFP fluorescence, confirming that phagemids containing the *GFP* gene could effectively generate the fluorescent protein. When sorting by FADS, almost all of the sorted droplets exhibited green fluorescence, indicating that these droplets contained the phagemids with *GFP* (Figure 2C,D). No green fluorescence was observed in the discarded droplets. These results demonstrated that FADS effectively enriched the droplets with superiority in phage synthesis and protected the phages from cross-contamination.

Cell-free PAE for screening the T7 RNAP to readthrough the T7 terminator

Since our optimized phagemids performed well in the cell-free system for M13 phage preparation and FADS, we investigated whether this system was suitable for directed evolution. To do so, we

Glossary

Cell-free synthesis system:

biochemical reaction system that facilitates *in vitro* protein synthesis and assembly, using exogenous mRNA or DNA as templates, along with enzymes, amino acid substrates, and energy sources to catalyze protein synthesis. This system encompasses the complete machinery for both transcription and translation. In concert with nucleic acid templates, these components enable protein synthesis devoid of the requirement for living cells.

Error-prone PCR (epPCR):

specialized PCR methodology using low-fidelity DNA polymerases to elevate the rate of base pair mismatches and introduce random mutations. This approach generates a spectrum of mutations comprising insertions, deletions, and base substitutions, thereby enhancing the diversity of the resultant PCR amplicons.

Fluorescence-activated droplet sorting (FADS):

high-throughput screening methodology that uses monodisperse microfluidic droplets to reduce enzyme reaction and screening systems to the picolitre scale, akin to the dimensions of a single cell. Directed by microfluidic chip technology, these droplets undergo rapid detection and precise sorting within designated microchannels.

M13 packaging signal (PS): specific DNA region in the genome of M13 phage that can fold into a hairpin structure, which serves as a recognition motif for DNA encapsulation. It is necessary for the initial assembly of M13 phage.

Origin of replication (ori): regulatory DNA sequence orchestrating the initiation of replication by specifically binding replication fork proteins, thereby initiating the replication process within plasmids or chromosomal DNA.

Phage-assisted evolution (PAE):

directed evolution strategy that leverages the rapid life cycle and operational simplicity of the phage. This approach enables the efficient and swift identification of high-performing mutants of GOI by manipulating the engineered phages that harbor GOI mutant libraries.

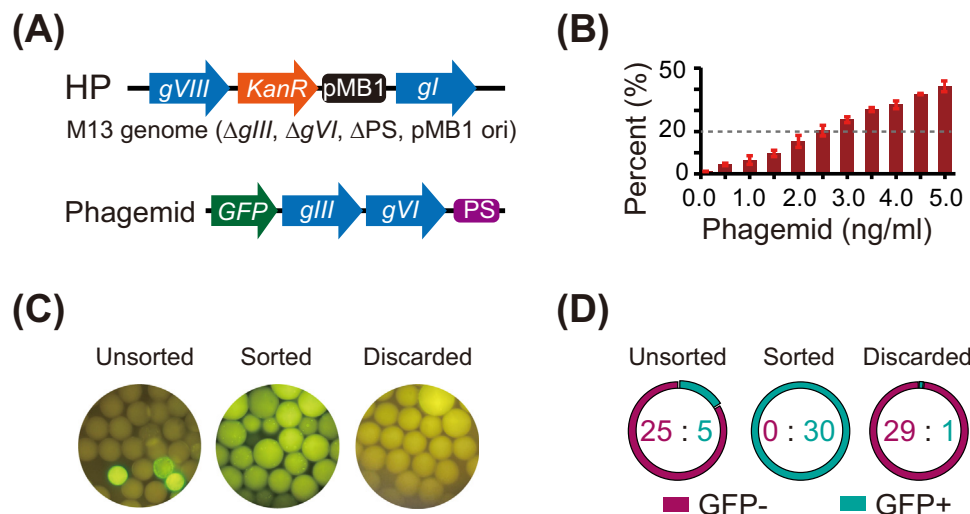


Figure 2. Developing a cell-free phage-assisted evolution (PAE) method in droplets. (A) Plasmids used in the cell-free PAE with a GFP sensor. (B) Percentage of fluorescent droplets after embedding with 0.1–5 ng/ml phagemid. (C) Fluorescence imaging to reveal sorting results. (D) Sanger sequencing to detect the number of wild-type and GFP phagemids. Error bars represent mean \pm standard deviation (SD). Abbreviations: HP, helper phage; ori, origin of replication; PS, packaging signal.

focused on the T7 RNAP, an important enzyme in directed evolution that is commonly used as a desirable GOI in genetic engineering and RNA synthesis [6].

Although the existing T7 RNAP has performed well in many applications, its extensibility remains hindered by some RNA structures, such as hairpin structures, which limit their transcription ability on complex DNA templates. To solve this problem, a specific reporter was designed to determine the ability of T7 RNAP to read through the T7 terminator (Figure 3A). In the phagemid, the gene VI (*gVI*) and *GFP* were designed as sensors located downstream of the expression cassette of the T7 promoter (P_{T7}) and terminator (T_{T7}).

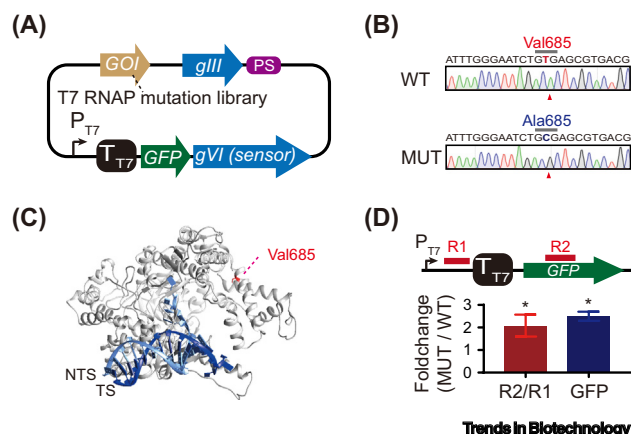


Figure 3. Using cell-free phage-assisted evolution (PAE) to screen T7 RNA polymerase (RNAP) mutants that read through the T7 terminator. (A) Plasmids used in the optimized cell-free phage production system for directed evolution of T7 RNAP. (B) Sanger sequencing detected the T7 RNAP mutation. (C) T7 RNAP structural analysis revealed the location of the Val685 residual in the T7 RNAP protein [Protein Data Bank (PDB) ID: 1CEZ]. The Val685 residual is in red, and the template (TS) and the nontemplate (NTS) strands are in blue. (D) RT-qPCR and GFP intensity assay to verify the fold-change in T7 RNAP Val685Ala mutants (MUT) to wild-type (WT) on reading through the T7 terminator. Region 1 (R1) represents the normal region, and region 2 (R2) represents the read-through region. Error bars represent mean \pm standard deviation (SD). An asterisk indicates that the data of these two groups have significant differences. Abbreviation: GOI, gene of interest; PS, packaging signal.

To efficiently and quickly obtain the widest possible library of mutants, we used **error-prone PCR (epPCR)** to construct in the phagemid a T7 RNAP mutant library at the C terminus (600–883), which contains the main active center of T7 RNAP [15,16]. After M13 phage generation and FADS, we obtained a T7 RNAP mutant of valine to alanine at residue 685 (Val685Ala), which was verified by Sanger sequencing (Figure 3B). The tertiary structural model showed that this residue is located near the nontemplate strand and the active center (Figure 3C). The mutation of valine to alanine may expand the range of inner channels in the enzyme, thus reducing the impediment of the hairpin structure to polymerase extension. Recent studies showed that there is a small cavity near the C terminus of T7 RNAP that is difficult for solvents to access, thus allowing for insertion of additional amino acid residues. Larger amino acid residues at the C terminus may reduce RNA production, which is similar to the phenomenon observed in our study [16].

Subsequently, we used the GFP reporter to determine the activity of T7 RNAP. RT-qPCR and GFP intensity assay results revealed a twofold increase in the ability of the Val685Ala mutant to read through the T7 terminator (Figure 3D). These results suggest that our cell-free phage synthesis system works well in directed evolution of T7 RNAP.

Cell-free PAE for screening suppressor tRNA

To further verify the efficiency of our cell-free PAE method, we focused on the suppressor tRNA, a specific tRNA that can recognize stop codons to continue the synthesis of the polypeptide chain as a desirable GOI [17]. We introduced a tryptophan nonsense mutation (UGG>UGA) in *gVI* and *GFP* in the phagemid as a sensor of the activity of suppressor tRNA (Figure 4A). A robust epPCR was also utilized to generate the random mutation library of *TrpT* of *E. coli* since there were no issues with frameshift mutations.

To verify the effect of FADS on enrichment of dominant mutants, we detected mutations in the process before and after FADS by using next-generation sequencing (NGS). Clustering analysis of the NGS data showed that the distribution of mutations in *TrpT* was similar in the samples before and after FADS, as well as showing a low correlation with the control sample (Figure 4B). The proportion of most mutations was downregulated during the two evolution processes, indicating the loss of function of these mutations (Figure 4C). Notably, only two mutations of *TrpT* were

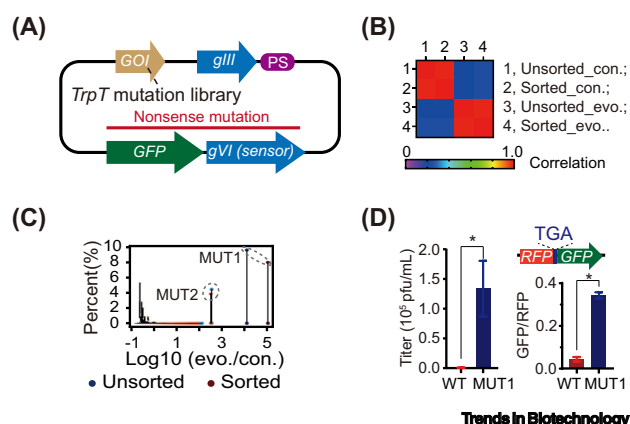


Figure 4. Using cell-free phage-assisted evolution (PAE) to screen tryptophan suppressor tRNA (TrpT). (A) Plasmids used in the optimized cell-free phage production system for directed evolution of TrpT. (B) Heatmap showing correlations between the next-generation sequencing (NGS) data of the control (con.) and evolved (evo.) samples before and after fluorescence-activated droplet sorting (FADS). (C) Volcano plot showing the correlation between the proportion of TrpT mutants (MUT) in evolved samples and the proportion change during evolution; the darker the color, the greater the fold change. MUT1 and MUT2 are highlighted by the gray-broken line box. (D) M13 phage titer and

dual-fluorescent protein reporting system assay to verify the effect of the TrpT mutant on reading through the UGA stop codon. Error bars represent means \pm standard deviation (SD). An asterisk indicates that the data of these two groups have significant differences. Abbreviation: pfu, plaque forming unit.

dramatically upregulated in both processes (MUT1 and MUT2). MUT1 exhibited an ~10 000-fold enrichment in the unsorted sample and >90 000-fold enrichment in the FADS-sorted sample (occupying ~8.0% of the sample) (Figure 4C). However, MUT2 exhibited an ~340-fold enrichment in the unsorted sample and an ~310-fold enrichment in the FADS-sorted sample (occupying ~3.9% of the sample) (Figure 4C). These results suggest that MUT1 has a higher performance as a tryptophan suppressor tRNA compared with MUT2, and that FADS could help to further improve the efficiency of directed evolution in this cell-free system.

We determined the activity of *TrpT* MUT1 suppressor tRNA by determining the titer of the M13 phage. Results revealed that these tryptophan tRNA mutations generated over 100 times more phages compared with wild-type by reading through the stop codon UGA (Figure 4D). We further used a dual-fluorescent protein reporting system [18] with a tryptophan nonsense mutation in *GFP* to detect the activity of evolved tRNA, and found that the GFP/RFP intensity of evolved tRNA was over eightfold higher than that of the wild-type (Figure 4D). These results suggest that our optimized cell-free phage production system can effectively screen for high-performance GOI mutants.

Discussion

Phage preparation technology is an important part of the phage application process. Traditional techniques rely on phage proliferation in fresh host strains, thus requiring tedious host culture and infestation steps for each phage preparation, limiting the efficiency of phage preparation [3,6]. In recent years, cell-free synthesis techniques have been widely used for protein and RNA preparation, and also have an important role in the assembly of non-membrane structures (e.g., ribosomes, transcriptional complexes, etc.) because they are considered to have greater potential for phage synthesis compared with traditional methods [9].

Unlike other phages produced by cell-free synthesis techniques [9,10], the genome of the M13 phage is ssDNA, with a rolling circle replication model [11]. Currently, there are no relevant reports on whether this replication mode can function in cell-free synthesis systems. Moreover, the individual aspect ratio of M13 phage is uneven (1000 nm:7 nm), which leads to an uneven protein copy number required for its assembly. Each M13 phage contains over 2000 copies of protein VIII but only a few copies of proteins VII and IX [11]. These factors may make the *in vitro* synthesis and assembly of M13 phage challenging [13]. When we used the full M13 genome as input, phage production was much lower than at the intracellular level. This suggests that although the rolling circle replication works well in the cell-free system, it is still inefficient for generating and assembling phage. A simplified genome can effectively improve phage synthesis by presynthesizing other genes by transforming them into the host strain earlier, especially in increasing the copy number of these presynthesizing genes, consistent with previous reports [12,13]. In our study, the synthesis ability of T7 phage was over 100 times higher than that of M13 phage, especially in cell-free systems, but comparable with that of the simplified M13 genome (data not shown). This study not only introduces a novel concept for the synthesis and assembly of complexes characterized by an imbalanced component distribution within cell-free systems, a phenomenon prevalent in various viral capsids [19], but also suggests that a reasonable protein copy number can maximize the assembly of mature M13 phage *in vitro*. Although our optimized *in vitro* M13 phage preparation method still produced phage titers slightly lower than those synthesized *in vivo*, phage preparation time and preparation efficiency were significantly improved, and no additional host cell culture was required. This provides new directions and ideas for the rapid preparation of M13 phage.

However, there is still no substitute for efficient preparation of phage *in vivo*, probably because the *in vivo* phage life cycle is able to maximize the exploitation of host material and energy to support phage synthesis, which is currently unattainable by *in vitro* preparation techniques [11].

Moreover, the cell-free phage synthesis method we developed has a faster synthesis rate compared with *in vivo* synthesis, suggesting that cell-free PAE will have a faster evolution rate than in cells. In addition, many enzymes and metabolic pathways are unsuitable for traditional PAE techniques due to the permeability of small molecules [20,21]. However, this problem can be solved in cell-free PAE. Nonetheless, cell-free PAE lacks continuous directed evolution due to its dependence on the compartmentalization of droplets to isolate mutants. This limitation can be effectively compensated for by combining powerful *in vitro* mutagenesis with the rapid screening dependent on phage proliferation. These findings indicate that cell-free PAE *in vitro* is an efficient and versatile directed evolution technique.

Although previous studies have attempted to utilize cell-free techniques to screen linear or plasmid DNA mutant libraries, they were hindered by the proliferation of DNA and sensing of mutant activity [22,23]. In this study, we exploited the phage self-propagation property in a cell-free system to facilitate the amplification of mutant DNA, and integrated the activity of mutant DNA with the phage self-propagation ability to achieve efficient rational mutant enrichment. By incorporating fluorescence-sensing technology and FADS, we significantly enhanced the enrichment efficiency of rational mutants during evolution. Ultimately, our cell-free phage synthesis technology demonstrated superior performance in evolutionary tests with T7 RNAP and suppressor tRNA.

Concluding remarks

Utilizing the CFPS platform, our research achieved two pivotal objectives. First, we refined a state-of-the-art methodology for M13 phage production within a cell-free synthesis system. This was accomplished through genome simplification and engineering, coupled with the presynthesis of multicopy proteins, thereby enabling the rapid and substantial generation of both M13 phage and its mutant library (see [Outstanding questions](#)). The M13 phage has been extensively applied across various fields, including biomedicine, diagnostics, therapeutics, and agriculture. A suite of practical technologies leveraging its lifecycle has been established, encompassing phage display, PAE, phage therapy, and the inhibition of environmental pathogens. Enhancing and streamlining the preparation process of phages can significantly reduce the complexity and improve the accessibility of these technologies, offering numerous benefits as well as savings in time and financial resources. The advancement and refinement of cell-free phage synthesis techniques have rendered the large-scale production of phages feasible, akin to the manufacturing processes for mRNA vaccines and pharmaceuticals.

Second, we developed a versatile cell-free PAE system in droplets, proficient at screening GOI mutants with enhanced performance. PAE has garnered significant attention within the realm of directed evolution, owing to its marked advantages of reduced time requirements, low cost, and high throughput, but is impeded by its intracellular life cycle. Our novel cell-free synthesis system in droplets adeptly overcomes this challenge, thereby amplifying the potential applications of PAE. We intend to harness this technology to identify a plethora of GOI mutants, with a particular focus on industrial enzymes that confer substantial economic advantages. This will encompass applications in gene-editing systems, pharmaceutical synthesis, food processing, biological carbon fixation, and the production of biofuels.

In summary, this novel M13 phage synthesis technology based on cell-free system represents a monumental leap forward in phage application technology. Its practicality and ease of use overcome the traditional reliance on cellular hosts, positioning it as a transformative instrument with the potential to profoundly impact multiple fields, including medicine, food processing, agriculture, and sustainable development.

Outstanding questions

How can the expression of various genes of the M13 phage be orchestrated in a cell-free synthesis system to augment the production and assembly capabilities of this phage?

Which strategies can be used to guarantee the integrity and stability of phage synthesized and assembled *in vitro*?

How can phage-assisted continuous evolution be facilitated within droplets?

Are these technologies developed for M13 phage applicable to a broader range of phages?

STAR★METHODS

Detailed methods are provided in the online version of this paper and include the following:

- KEY RESOURCES TABLE
- METHOD DETAILS
 - Strains and plasmids
 - Titer determination of M13 phage
 - Cell-free phage production
 - Construction of mutant phage libraries
 - Droplet preparation and FADS
 - Next generation sequencing
 - Activity assay of T7 RNA polymerase
 - Activity assay of suppressor tRNA
- QUANTIFICATION AND STATISTICAL ANALYSIS

RESOURCE AVAILABILITY

Lead contact

Further information and requests for resources should be directed to and will be fulfilled by the lead contact, Ao Jiang (jiangao@tidetronbio.com).

Materials availability

Plasmids constructed in this study are listed in the STAR★METHODS.

Data and code availability

All data generated or analyzed during this study are included in this published article.

Author contributions

Conceptualization: B.X., A.J.; methodology: B.X., L.H.L., H.L.L., Y.Z.; validation: L.H.L., Y.H., Q.H., F.W.; formal analysis: B.X., A.J.; resources: B.X., Y.R.W., Z.Q.Z.; writing: B.X., A.J.; supervision: B.X.; project administration: B.X.; and funding acquisition: B.X., Z.Q.Z..

Acknowledgments

Support for this work was provided by the Hubei University of Science and Technology Program (No. BK202417).

Declaration of interests

The authors declare that they have no known competing financial interests or personal relationships that could have appeared to influence the work reported in this article.

Declaration of generative AI and AI-assisted technologies in the writing process

During the preparation of this work, the authors used ChatGPT in order to improve the readability and quality of the text. After using this tool, the authors reviewed and edited the content as needed and take full responsibility for the content of the publication.

Supplemental information

Supplemental information to this article can be found online at <https://doi.org/10.1016/j.tibtech.2024.10.005>.

References

1. Strathdee, S.A. *et al.* (2023) Phage therapy: from biological mechanisms to future directions. *Cell* 186, 17–31
2. Yehl, K. *et al.* (2019) Engineering phage host-range and suppressing bacterial resistance through phage tail fiber mutagenesis. *Cell* 179, 459–469
3. Saw, P.E. and Song, E.W. (2019) Phage display screening of therapeutic peptide for cancer targeting and therapy. *Protein Cell* 10, 787–807
4. Schmitt, D.S. *et al.* (2024) Applications of designer phage encoding recombinant gene payloads. *Trends Biotechnol.* 42, 326–338
5. Kocot, A.M. *et al.* (2023) Phages and engineered lysins as an effective tool to combat Gram-negative foodborne pathogens. *Compr. Rev. Food Sci. Food Saf.* 22, 2235–2266
6. Esvelt, K.M. *et al.* (2011) A system for the continuous directed evolution of biomolecules. *Nature* 472, 499–503
7. Brodel, A.K. *et al.* (2016) Engineering orthogonal dual transcription factors for multi-input synthetic promoters. *Nat. Commun.* 7, 13858
8. Al'Abri, I.S. *et al.* (2022) Inducible directed evolution of complex phenotypes in bacteria. *Nucleic Acids Res.* 50, e58

9. Levrier, A. *et al.* (2024) PHEIGES: all-cell-free phage synthesis and selection from engineered genomes. *Nat. Commun.* 15, 2223
10. Emslander, Q. *et al.* (2022) Cell-free production of personalized therapeutic phages targeting multidrug-resistant bacteria. *Cell Chem. Biol.* 29, 1434–1445
11. Smeal, S.W. *et al.* (2017) Simulation of the M13 life cycle I: assembly of a genetically-structured deterministic chemical kinetic simulation. *Virology* 500, 259–274
12. Brodel, A.K. *et al.* (2017) Intracellular directed evolution of proteins from combinatorial libraries based on conditional phage replication. *Nat. Protoc.* 12, 1830–1843
13. Wickner, W. and Killick, T. (1977) Membrane-associated assembly of M13 phage in extracts of virus-infected *Escherichia coli*. *Proc. Natl. Acad. Sci. U. S. A.* 74, 505–509
14. Baret, J.C. *et al.* (2009) Fluorescence-activated droplet sorting (FADS): efficient microfluidic cell sorting based on enzymatic activity. *Lab Chip* 9, 1850–1858
15. Maksimova, T.G. *et al.* (1991) Lys631 residue in the active site of the bacteriophage T7 RNA polymerase. Affinity labeling and site-directed mutagenesis. *Eur. J. Biochem.* 195, 841–847
16. Douxis, A. *et al.* (2023) An engineered T7 RNA polymerase that produces mRNA free of immunostimulatory byproducts. *Nat. Biotechnol.* 41, 560–568
17. Albers, S. *et al.* (2023) Engineered tRNAs suppress nonsense mutations in cells and in vivo. *Nature* 618, 842–848
18. DeBenedictis, E.A. *et al.* (2021) Multiplex suppression of four quadruplet codons via tRNA directed evolution. *Nat. Commun.* 12, 5706–5718
19. Mateu, M.G. (2013) Assembly, stability and dynamics of virus capsids. *Arch. Biochem. Biophys.* 531, 65–79
20. Miller, S.M. *et al.* (2020) Phage-assisted continuous and non-continuous evolution. *Nat. Protoc.* 15, 4101–4127
21. Roth, T.B. *et al.* (2019) Phage-assisted evolution of *Bacillus methanolicus* methanol dehydrogenase 2. *ACS Synth. Biol.* 8, 796–806
22. Sieskind, R. *et al.* (2023) Cell-free production systems in droplet microfluidics. *Adv. Biochem. Eng. Biotechnol.* 185, 91–127
23. Holstein, J.M. *et al.* (2021) Cell-free directed evolution of a protease in microdroplets at ultrahigh throughput. *ACS Synth. Biol.* 10, 252–257
24. Bolger, A.M. *et al.* (2014) Trimmomatic: a flexible trimmer for Illumina sequence data. *Bioinformatics* 30, 2114–2120

STAR★METHODS

KEY RESOURCES TABLE

Reagent or resource	Source	Identifier
Bacterial and phage strains		
<i>Escherichia coli</i> JM109	Beyotime Biotech	Cat#D1047S
<i>E. coli</i> BL21(DE3)	TransGen Biotech	Cat#CD601-02
Critical commercial assays		
High-Fidelity DNA Polymerase	Yeasen Biotech	Cat#10140
One Step Cloning Kit	Yeasen Biotech	Cat#10922
QuickMutation Random Mutagenesis Kit	Beyotime Biotech	Cat#D0219S
Ultima DNA Library Prep Kit	Yeasen Biotech	Cat#12199
DNA Selection Beads	Yeasen Biotech	Cat#12601
Phage DNA Isolation Kit	AmyJet Scientific	Cat#46822
One Step RT-qPCR SYBR Green Kit	Yeasen Biotech	Cat#11143
Bacteria Total RNA Isolation Kit	Sangon Biotech	Cat#B518625
Recombinant DNA		
M13KO7-ΔPS-ΔgIII-ΔgVI	Brodel <i>et al.</i> [12]	Addgene Plasmid #80840
Phagemid	Brodel <i>et al.</i> [12]	Addgene Plasmid #80852
pJPC12-ΔPS-PRM-B0034-geneVI	Brodel <i>et al.</i> [12]	Addgene Plasmid #80858
Software and algorithms		
Trimmomatic	Bolger <i>et al.</i> [24]	https://github.com/usadellab/Trimmomatic
GraphPad Prism 10.0	GraphPad Software	https://www.graphpad.com/
RNAfold	RNAfold Software	http://rna.tbi.univie.ac.at/cgi-bin/RNAWebSuite/RNAfold.cgi

METHOD DETAILS

Strains and plasmids

The plasmid of M13KO7-ΔPS-ΔgIII-ΔgVI (addgene #80840), phagemid (addgene #80852), and accessory plasmid pJPC12-ΔPS-PRM-B0034-geneVI (addgene #80858) were purchased from Addgene. The gene of RFP-TGA was synthesized from IGE Biotech and constructed into the downstream of GFP start codon of pT7-GFP plasmid to fused into a RFP-TGA-GFP gene. The DNA of gene VI was amplified using the primer pair gVI-F/R and the template of pJPC12-ΔPS-PRM-B0034-geneVI. Similarly, the DNA of tRNA was amplified using the primer pair tRNA-F/R and the genome template from *E. coli* BL21(DE3). The DNA of T7 RNAP was amplified using the primer pair T7-F/R and the genome template from *E. coli* BL21(DE3). The nonsense mutation of gene VI in accessory plasmid was amplified using the primer pair AP-F/R and the plasmid template of pJPC12-ΔPS-PRM-B0034-geneVI. These genes were amplified by using Hieff Canace® Plus High-Fidelity DNA Polymerase (Yeasen Biotech) and the corresponding primers as listed below. Plasmids were constructed using Hieff Clone® Plus One Step Cloning Kit (Yeasen Biotech) and the corresponding DNA fragment.

gVI-F: 5'-ttgctaacatactgcgtaataaggagtcttaatcatgccagttctttgggtattccgttattattgcg-3';

gVI-R: 5'-ccttcgttttatttgatgcctgggtcttcttatttatccaatccaaataagaaacg-3';

phagemid1-F: 5'-cgcaataataacggaatacccaaaagaactggcatgattaagactccttattacgcagtatgtagc-3';

phagemid1-R: 5'-cgtttctatttggattgggataaataagaagaccagcatcaaataaaacgaaagg-3';

tRNA-F: 5'-tgcgtaataaggagctttaagaagacccccggtagcggttagtcagtcggttagaataacc-3';

tRNA-R: 5'-gccacagctcttcgactgagccttcgtttatttgatgcctctggcaaggatgccggtagaaggatttac-3';

T7-F: 5'-atgaacacgattaacatcgctaagaacgac-3';

T7-R: 5'-ttacgcgaacgcgaagtcgactc-3';

phagemid2-F: 5'-gtaaatccttctaccggcatccttgccagaggcatcaataaaacgaaaggctcagtcgaaagactg-ggc-3';

phagemid2-R: 5'-caggtattctaaccgactgaactaccgctccaccgggtcttottaagactccttattacgcagtatgtt-agc-3';

AP-F: 5'-attgggtaccgggcccacaatgtatcttgaagaggagaaatactagatgTGATGAccagttctttgggta-ttccgttattatgcg-3';

AP-R: 5'-taataacggaatacccaaaagaactggTCATCAcatctagttatttctcctctttacaagatacattgtgggcc-cggtacccaattcgcc-3';

GFP-F: 5'-ttgtttaactttaagaaggagatatacatatgTGAagcaaagggtgaagaactgttaccg-3';

GFP-R: 5'-cggtaaacagttcttcaccttgcctTCACatattgtatatctcctcttaagtaaacaaa-3'.

Titer determination of M13 phage

The *E. coli* JM109 strain harboring M13KO7- Δ PS- Δ gIII- Δ gVI was cultivated at an OD600 value of 0.4-0.6 at 37 °C in 2× YT broth (20 g/l Tryptone, 10 g/l Yeast extract, and 10 g/l sodium chloride) with 50 mg/l kanamycin. LB agar plates containing 1.5% agar and 50 mg/l kanamycin were used as the bottom layer. Serial dilutions of the phage sample were prepared in sterile LB broth. In a sterile tube, mix 10 μ l of the diluted phage with 1 ml of the bacterial host culture, and then allow the mixture to incubate at room temperature for 10 minutes to facilitate phage adsorption. LB agar containing 0.7% agar and 50 mg/l kanamycin was melted and kept in a liquid state at 50°C in a water bath. Add 6 ml of the pre-warmed soft agar to the phage-bacteria mixture, and stir gently but thoroughly. Immediately pour this mixture over the surface of a prepared LB agar plate. Swirl the plate to distribute the soft agar evenly. Let the top agar solidify at room temperature. Invert the plates and incubate at 37°C for 12 hours. After incubation, count the number of plaques (clear zones) on each plate. Select plates with 30-300 plaques for accurate counting. The phage titer is calculated in plaque-forming units per mL (pfu/ml) using the formula: Titer (pfu/ml) = (Number of plaques) \times (Dilution factor) / (Volume of phage sample).

Cell-free phage production

The *E. coli* JM109 cells harboring the HP plasmid were grown in a 5 l bioreactor with pO₂ monitoring and pH control. At the optimal growth phase, the culture was harvested during the mid-log phase, then washed and immediately flash-frozen in liquid nitrogen. It was subsequently stored overnight at -80°C. The following day, the pellet was carefully thawed on ice and resuspended. Cell disruption was achieved through a combination of lysozyme treatment and sonication, followed by centrifugation. Subsequently, the cells were incubated at 37°C, leading to a second centrifugation. Finally, the resulting cell lysate was dialyzed, subjected to another round of centrifugation, and then flash-frozen in liquid nitrogen, to be stored at -80°C until further use.

Phage synthesis and assembly were assembled according to previous reported [10]. Specifically, the stock buffer is composed of: 6 mM Mg-glutamate, 20 mM K-glutamate, 2 mM DTT, 1.5 mM each amino acid, 50 mM HEPES, 1.5 mM ATP and GTP, 0.9 mM CTP and UTP, 0.2 mg/mL tRNA, 0.26 mM CoA, 0.33 mM NAD, 0.75 mM cAMP, 0.068 mM folinic acid, 1 mM spermidine, 30 mM 3-PGA, 3% PEG-8000, pH 8. The cell-free reaction mixture contained 330 μ l of *E. coli* crude extract, 7 μ l of PEG-8000, 30 μ l of dNTPs (25 mM), 10 μ l of ATP (500 mM), 300 μ l of stock buffer, 15 μ l of GamS (150 mM), and 100 ng of DNA, and was carried out at 30°C in a total volume of 1 ml.

Construction of mutant phage libraries

The mutation library of *T7 RNAP* and *TrpT* gene were constructed by error-prone PCR using the QuickMutation Random Mutagenesis Kit (Beyotime), according to the instruction manual. Specifically, for *T7 RNAP* gene, the target region was the C-terminal (600–883) of

T7 RNAP protein, and the primer used to amplify the fragment were T7MUT-F (5'-gaccgatgagaacactggtgaaatctctgag-3') and T7MUT-R (5'-cgcgaaacgcgaagtcgactctaagatgac-3'). A 0.5× Mutation enhancer was used to minimize the undesirable insertions and deletions. For the *TrpT* gene, the entire DNA was amplified using tRNA-F/R primers. A 5× Mutation enhancer was used to generate as complex a mutation library as possible.

The mutation libraries of the *T7 RNAP* and *TrpT* gene were separately cloned into the M13 genome skeleton using the Hieff Clone® Plus One Step Cloning Kit (Yeasten Biotech). The cloning product was purified by Hieff NGS® DNA Selection Beads (Yeasten Biotech), and then added to the cell-free system. After incubated at 30°C overnight, the phage was obtained from the supernatant. The mutation abundance in the library was verified by Sanger sequence after titer determination.

Droplet preparation and FADS

The fabrication of microfluidic chips using poly(dimethylsiloxane) (PDMS, Dow Corning Corp.) was achieved employing standard soft-lithography techniques. In our setup, a dropmaker chip generated 20 pL droplets at 4000 Hz by flow-focusing the cell-free synthesis system (5 µL/min) with two streams of HFE7500 fluorinated oil (3M) (10 µL/min) containing 4w/w% FluoSurf surfactant. After their generation, the droplets were directed off-chip through PTFE tubing to a collector. These droplets were then incubated at 30°C for 6 hours. In the subsequent phase, droplets were reloaded at 0.2 µL/min and spaced with HFE7500 fluorinated oil (3M) at 1 µL/min. Here, the droplets were detected and analyzed by the optical setup, with fluorescent droplets being sorted at 500 Hz using an AC field pulse (30 kHz; 700–1000 V; 0.5 ms). Finally, sorted droplets were collected in a 1.5 mL microcentrifuge tube. By contrast, in the analysis mode, the reloading module operated similarly, with droplets being detected and analyzed at approximately 1000 Hz.

Next generation sequencing

After evolution, the phage in droplet was extracted by adding Drop-Surf emulsifier (FluidicLab) and subsequently amplified in the *E. coli* strain JM109 containing the HP. Phages were collected from the culture supernatant, and their DNA was extracted using the Phage DNA Isolation Kit (AmyJet Scientific). The concentration and quality of the extracted RNA were detected used NanoDrop (ThermoFisher).

Next, the DNA fragment of the *TrpT* gene was amplified by using High Fidelity DNA Polymerase (Yeasten Biotech) with the tRNA-F/R primers. The input of phage DNA was 100 ng, and the PCR cycle number was 5. The PCR product was purified using Hieff NGS® DNA Selection Beads (Yeasten Biotech), and the DNA library was constructed using Hieff NGS® Ultima DNA Library Prep Kit for Illumina (Yeasten Biotech). The DNA library was sequenced on the Illumina NovaSeq 6000 platform with the PE150 model.

After sequencing, the adaptors at both end of the sequencing reads were trimmed using Trimmomatic (<https://github.com/usadellab/Trimmomatic>) [24]. This was followed by the assembly of Reads 1 and Reads 2 into complete sequences, which were then mapped to the *TrpT* gene. The types of mutations and their abundances were subsequently calculated and analyzed.

Activity assay of T7 RNA polymerase

The *E. coli* strain JM109, containing the HP and P_{T7} - T_{T7} -GFP plasmids, was cultured in the 2× YT medium at 37°C until the OD600 value reached 0.4. Subsequently, a titer of 10^6 pfu/mL phages carrying the T7 RNAP of wildtype and Val685Ala mutation were added to 1 mL of fresh culture and incubated at 37°C and 100 rpm for 6 h.

The GFP intensity was measured using a fluorescent microplate reader (Tecan). Following this, total RNA was extracted using the Bacteria Total RNA Isolation Kit (Sangon Biotech), and the concentration and quality of extracted RNA were assessed using NanoDrop (ThermoFisher). To measure the activity of T7 RNAP to read through T7 terminator, RT-qPCR was employed to measure the RNA level of the regions upstream and downstream of the T7 terminator, by using the Hifair® III One Step RT-qPCR SYBR Green Kit (Yeasten Biotech). The RNA of the upstream region was amplified with the primers (up-F: 5'-gacacggatgtactcaaagcggac-3'; up-R: 5'-tgcaacggtcagtttgccctg-3'), and the RNA of downstream region was amplified with the primers (up-F: 5'-ggcagtgctgcagctggcag-3'; up-R: 5'-cagaacggctctgcgtgctcag-3').

Activity assay of suppressor tRNA

The activity of suppressor tRNA was determined by the phage titer and GFP intensity, both of which containing the nonsense mutation UGA in the cell-free system. Briefly, for the phage titer determination, the accessory plasmid contains gVI with two nonsense

Statistical analyses were performed using the GraphPad Pr